

- Husfeld, J. A. Love, *Org. Lett.* **1999**, *1*, 137; see also: i) S. R. Gilbertson, G. S. Hoge, *Tetrahedron Lett.* **1998**, *39*, 2075; j) P. Binger, P. Wedemann, S. I. Kozhushkov, A. de Meijere, *Eur. J. Org. Chem.* **1998**, 113.
- [3] a) B. M. Trost, F. D. Toste, H. Shen, *J. Am. Chem. Soc.* **2000**, *122*, 2379; b) B. M. Trost, H. C. Shen, *Org. Lett.* **2000**, *2*, 2523.
- [4] For a comprehensive review, see: S. A. Godleski in *Comprehensive Organic Synthesis, Vol. 4* (Eds.: B. M. Trost, I. Fleming, M. F. Semmelhack), Pergamon, Oxford, **1999**, chap. 3.3, pp. 585–662.
- [5] M. P. Doyle, K.-L. Loh, K. M. De Vries, M. S. Chinn, *Tetrahedron Lett.* **1987**, *28*, 833.
- [6] M. W. Miller, C. R. Johnson, *J. Org. Chem.* **1997**, *62*, 113.
- [7] J. d'Angelo, *Tetrahedron* **1976**, *32*, 2979, and references therein.
- [8] B. M. Trost, B. Vidal, M. Thommen, *Chem. Eur. J.* **1999**, *5*, 1055, and references therein.
- [9] P. A. Jacobi, K. Lee, *J. Am. Chem. Soc.* **2000**, *122*, 4295.
- [10] For a similar mechanistic proposal in the Rh-catalyzed reaction, see ref. [2].

Correlating Electron Transport and Molecular Structure in Organic Thin Films**

R. Erik Holmlin, Rustem F. Ismagilov, Rainer Haag, Vladimiro Mujica, Mark A. Ratner, Maria Anita Rampi,* and George M. Whitesides*

Understanding how electrons travel through organic matter is important in designing materials for organic microelectronics^[1] and understanding biological electron-transport processes.^[2,3] Herein we describe a simple experimental procedure to measure rates of electron transport across organic thin films having a range of structures, compare the data for several types of films, and outline a theory appropriate for analyzing these rates. We use a junction that is particularly easy to assemble: M-SAM(1)SAM(2)-M' (Figure 1, "SAM" is a self-assembled monolayer).^[4,5] We have

[*] Prof. M. A. Rampi
 Dipartimento di Chimica, Centro di Fotochimica CNR, Università di Ferrara, 44100 Ferrara (Italy)
 Fax: (+39)0532240709
 E-mail: rmp@unife.it

Prof. G. M. Whitesides, Dr. R. E. Holmlin, Dr. R. F. Ismagilov, Dr. R. Haag
 Department of Chemistry and Chemical Biology, Harvard University, Cambridge, MA 02138 (USA)
 Fax: (+1) 617-495-9857
 E-mail: gwhitesides@gmwgroup.harvard.edu

Dr. V. Mujica, Prof. M. A. Ratner
 Department of Chemistry, Northwestern University, Evanston, IL 60208 (USA)

[**] This work was supported by the Office of Naval Research, the Defense Advanced Research Project Agency, and the National Science Foundation ECS-97294053. R.E.H. thanks the National Institutes of Health for a postdoctoral fellowship, and R.H. thanks the Deutsche Forschungsgemeinschaft and the BASF fellowship program for financial support. We thank Andreas Terfort for the synthesis of aromatic thiols. Collaboration between Caracas and Evanston is supported by NSF Conicet.

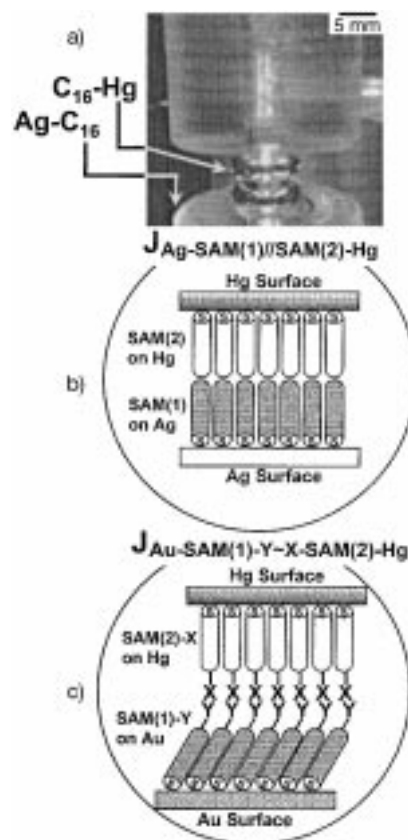


Figure 1. Schematic illustrations of junctions with structures $J_{\text{Ag-SAM}(1)/\text{SAM}(2)\text{-Hg}}$ and $J_{\text{Au-SAM}(1)\text{-Y-X-SAM}(2)\text{-Hg}}$ (see text for the nomenclature). The photographic image (a) is that of a $J_{\text{Ag-C}_{16}/\text{C}_{16}\text{-Hg}}$ junction; the scale bar represents ~ 0.5 mm. To assemble $J_{\text{Ag-SAM}(1)/\text{SAM}(2)\text{-Hg}}$ junctions (b), a SAM was formed on the surface of a thin evaporated film of silver; we normally used $M = \text{Ag}$, since silver gives highly ordered SAMs.^[5] This electrode was covered with a solution of hexadecane containing 1 mM thiol. A small drop of Hg (5 μL) was expressed into a solution of hexadecanethiol (HDT) from a capillary connected to a mercury reservoir, and a SAM of HDT allowed to form on it.^[5] The HDT-covered mercury drop ($\text{C}_{16}\text{-Hg}$) was then brought into contact with the solid electrode using a micromanipulator. The area of interfacial contact was estimated by using a microscope. With each electrode connected to an electrometer (in two-electrode mode), we applied a potential and recorded the response, and then increased the potential in steps over a range of voltages to generate I - V curves. Junctions of structure $J_{\text{Au-SAM}(1)\text{-X-Y-SAM}(2)\text{-Hg}}$ (c) were made as described for $J_{\text{Ag-SAM}(1)/\text{SAM}(2)\text{-Hg}}$ except that one electrode was a thin film of gold, and the thiols used had terminal groups that could react and form covalent bonds ($X = \text{carboxylic anhydride}$, $Y = \text{H}_2\text{N}$),^[15] or interact strongly but noncovalently ($X = \text{CO}_2\text{H}$ and $Y = \text{HO}_2\text{C}$, or $X = \text{CO}_2\text{H}$ and $Y = \text{H}_2\text{N}$) through hydrogen or ionic bonds.

examined two sets of junctions: 1) one in which SAM(1) was formed on Ag from aliphatic or aromatic thiols, and SAM(2) was formed on Hg from hexadecanethiol, and 2) a second in which SAM(1) and SAM(2) have terminal functional groups. In the first, the SAMs contact through van der Waals interactions; in the second, through covalent, hydrogen, or ionic bonds. The current measured across these junctions obeyed the relation $I = I_0 e^{-\beta d}$ (where d is the distance between the electrodes, and β is the structure-dependent attenuation factor for the molecules in SAM(1)); the values of β compare well with those obtained by other experimental methods. The experimental current versus voltage (I - V) curves have been fitted using two theoretical models for electron transport: one

based on tunneling through an unstructured barrier with a parabolic profile, and the second based on “superexchange” tunneling through molecules. These models generate values of β and potential barrier that are internally consistent and comparable with relevant information in the literature. Measurements of current across these junctions as a function of the structure of the SAMs provide information fundamental to understanding electron transport in organic matter.

We describe the two types of junctions we have studied (Figure 1) by using a nomenclature in which J indicates a junction: for the first, $J_{M-SAM(1)/SAM(2)-Hg}$, // represents van der Waals interactions at the interface between methyl-terminated SAMs; for the second, $J_{M-SAM(1)-X\sim Y-SAM(2)-Hg}$, \sim represents covalent, hydrogen, or ionic bonds that bridge the interfaces through functional groups X and Y. We use — for covalent bonds, and \cdots for hydrogen or ionic bonds. The procedure used to assemble the junctions was straightforward (Figure 1, caption). Current was measured in response to a fixed applied potential across the junction.^[5] Most junctions were stable for applied potentials over the range 0–1 V;^[5] 1 V corresponds to a potential gradient of approximately 10^8 V m⁻¹, well below the breakdown voltage of the system.^[5]

Junction 1: Figure 2a shows the current density across junctions with the structure $J_{Ag-SAM(1)/SAM(2)-Hg}$ as a function of

applied voltage for SAMs of alkanethiols, $HS(CH_2)_{n-1}CH_3$ ($n=8,10,12,14,16$), oligophenylene thiols, $HS(Ph)_kH$ ($k=1,2,3$), and benzylic homologues of the oligophenylene thiols $HSCH_2(Ph)_mH$ ($m=1,2,3$). Comparison of these I – V curves, and of their fits to theoretical models (described below) indicate that: a) the *shape* of the I – V curves is the same for C_n , Ph_kH , and CH_2Ph_mH ; b) the magnitude of the current density decreases in the order $Ph_kH > CH_2Ph_mH > C_n$ for films of the same thickness; c) the magnitude of the current density depends on the thickness of the monolayers. The decrease in current density with increasing distance separating the electrodes ($d_{Ag,Hg}$) obeyed the relation $I = I_0 e^{-\beta d_{Ag,Hg}}$, as expected for tunneling (Figure 2b). For alkanethiols forming SAM(1) on Ag, β is 0.87 ± 0.1 Å⁻¹; for oligophenylene thiols, β is 0.61 ± 0.1 Å⁻¹; and for the benzylic derivatives of oligophenylene thiols, β is 0.67 ± 0.1 Å⁻¹.

The value of β is approximately independent of V (over the range 0.1–1 V). This observation suggests that the molecular bridge states, which determine the effective pathway of transport, are weakly sensitive to voltage changes in the range considered. We assumed that any scattering of electrons at the interface between the SAMs was the same for aliphatic and aromatic SAMs. These values of β are in good agreement with corresponding values obtained by photoinduced electron transfer in molecular systems comprising electron donor and

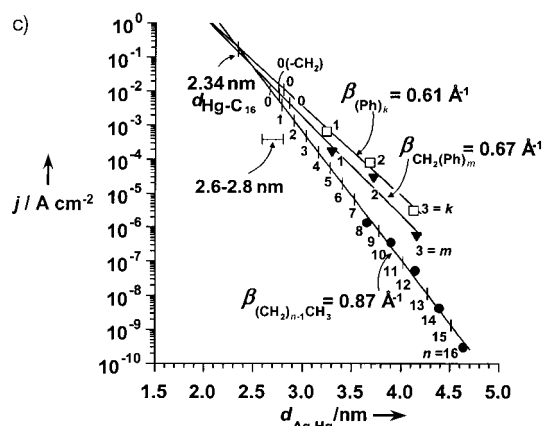
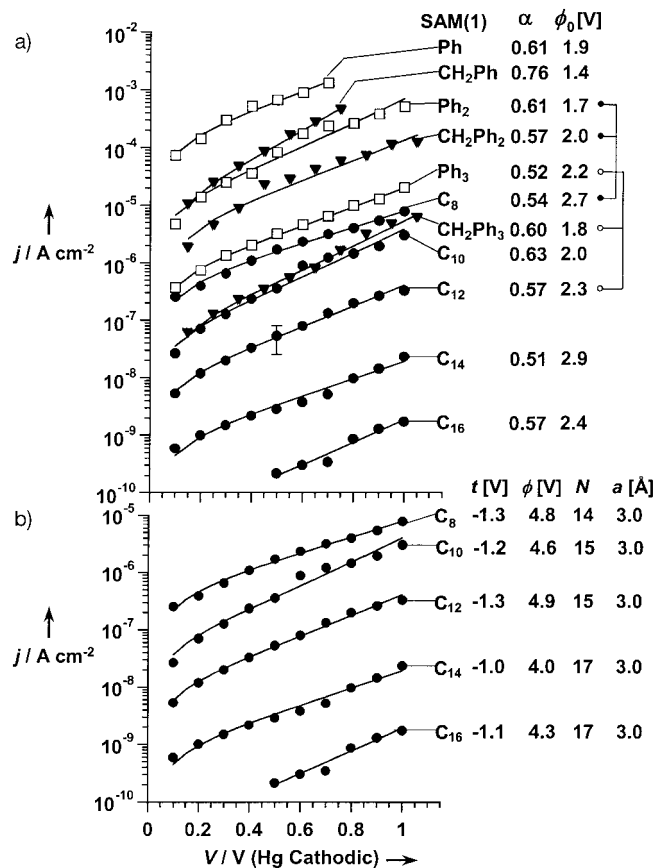


Figure 2. a) Plots of current density j as a function of the bias voltage V between the mercury and silver electrodes for $J_{Ag-SAM(1)/C_{16}-Hg}$. The symbols used to represent different classes of compounds are: ●, $HS(CH_2)_{n-1}CH_3$; □, $HS(Ph)_kH$ (all substitution of benzene rings is 1,4); ▼, $HSCH_2(Ph)_mH$. The solid lines represent the best nonlinear, least-squares fits of the data for each junction to Equation (1); all points were weighted equally, and the equation had two floating parameters, ϕ_0 and α . The correlation coefficient (R^2) for each was >0.95 . We list the value of ϕ_0 and α obtained by these fittings. The lines connecting triads of data adjacent to values of ϕ_0 and α are for SAMs on Ag having the same thickness. To test the statistical significance of our inference that the magnitude of the current density decreases in the order $Ph_k > CH_2Ph_m > C_n$ for films of the same thickness, we examined the curves for Ph_2 and CH_2Ph_2 . Application of the Student's t -test indicated that, for uncertainties of the size shown, $I(Ph_2) > I(CH_2Ph_2)$ ($V=0.1-1$) at $>95\%$ confidence level. Other comparisons are even more

certain. The error bar in a) is \pm the standard deviation of the data, s ; each datum is the average of six measurements on six independent junctions. b) Plot of current density j as a function of the bias voltage V (solid circles) for junctions with composition for $J_{Ag-C_n/C_{16}-Hg}$ ($n=8,10,12,14,16$). The solid lines represent the best nonlinear, least-squares fits of the data for each junction to Equation (3); all points were weighted equally. Each line in this figure is a fit to Equation (3) using four floating parameters. c) Plot correlating values of current density and distance between electrodes for $J_{Ag-SAM(1)/C_{16}-Hg}$ at $V=0.5$ V. The lines are linear least-squares fits to the equation $\ln(I) = -\beta d + \ln(I_0)$.

acceptor linked by a bridge^[6, 7] and by electron transfer between a solid electrode and redox-active species in solution.^[8] In these systems, values of β for saturated hydrocarbons range from 0.8–1.0 Å⁻¹,^[6, 8] and values of β for oligophenylenes range from 0.4–0.6 Å⁻¹.^[7, 9] In directly comparable work, Majda and co-workers found $\beta = 0.8 \pm 0.1 \text{ \AA}^{-1}$ for alkanethiols in $J_{\text{Hg-SAM}/\text{SAM-Hg}}$.^[10] The agreement among the values of β suggests that the mechanism of charge transport in these solid-state junctions is closely related to that in molecular systems in solution, and that across SAMs on solid electrodes to molecules in solution in electrochemical experiments.

Figure 2c summarizes an analysis that establishes the internal consistency of the data for the three sets of junctions, $J_{\text{Ag-S(CH}_2)_n\text{-CH}_2/\text{C}_{16}\text{-Hg}}$, $J_{\text{Ag-(Ph)}_k/\text{C}_{16}\text{-Hg}}$, and $J_{\text{Ag-CH}_2(\text{Ph})_m/\text{C}_{16}\text{-Hg}}$. We extrapolated plots of current density against $d_{\text{Ag,Hg}}$ for each of the three junctions to their intersection points (where, in principle, there is no contribution to the junctions from an organic monolayer on silver). The thickness calculated for the hypothetical junction $J_{\text{Ag}/\text{C}_{16}\text{-Hg}}$ is $d_{\text{Ag,Hg}} = 2.34 \text{ nm}$; that for a junction in which the organic groups on silver had been removed, and only the Ag–S bond and the van der Waals radius of the terminal methyl group or hydrogen atom remain is $d_{\text{Ag,Hg}} = 2.6–2.8 \text{ nm}$. The difference between 2.34 nm and 2.6–2.8 nm—0.3–0.5 nm—is a reasonable value for an aggregate contribution to the thickness from the Ag–S bond, the S–C bond, and the van der Waals radii of the terminal groups. The consistency of our data for the three sets of organic compounds suggests that they are directly comparable.

Junction 2: Comparisons of rates of electron transfer through different types of covalent bonds and through nonbonding interactions have been challenging^[11] and only a few have been reported.^[12–14] Assembling a junction by bringing together two metal surfaces coated with SAMs that terminate in different functional groups (X and Y) makes it straightforward to incorporate a variety of interactions into the junction $J_{\text{Au-SAM(1)-X~Y-SAM(2)-Hg}}$; we have compared van der Waals interactions and hydrogen or hydrogen/ionic bonds (Figure 3). It was also possible to bridge two SAMs covalently by reaction of a SAM terminated with anhydride groups on gold with a second SAM terminated in amine groups on

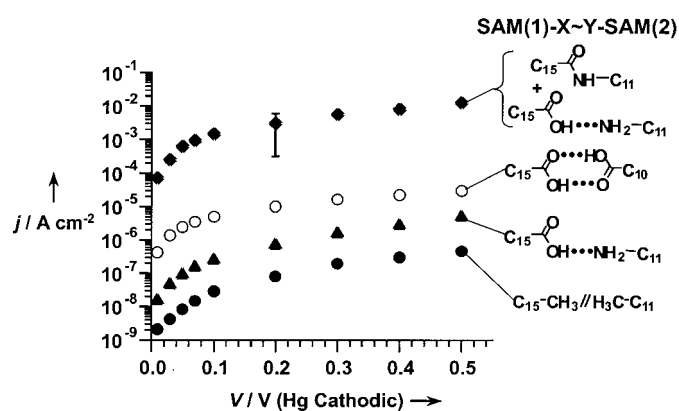


Figure 3. Plots of current density as a function of the bias voltage between the mercury and gold electrodes for $J_{\text{Au-SAM(1)-X~Y-SAM(2)-Hg}}$. The error bar is \pm the standard deviation of the data, s .

mercury.^[15] This reaction generates a 1:1 mixture of two kinds of bridging groups: covalent amide C(O)–NH groups and hydrogen-bonded $\text{CO}_2\text{H}\cdots\text{NH}_2$ pairs.

The current density measured at a particular value of applied voltage depended significantly on the structure of the interface. Using the junction having only van der Waals interactions at the interface as the reference, $I_{(-\text{CO}_2\text{H}\cdots\text{NH}_2)}/I_{(-\text{CH}_3/\text{H}_3\text{C})} \approx 9$; $I_{(-\text{CO}_2\text{H}\cdots\text{HO}_2\text{C})}/I_{(-\text{CH}_3/\text{H}_3\text{C})} \approx 40$; and $I_{(-\text{C(O)NH}\cdots\text{CO}_2\text{H}\cdots\text{NH}_2)}/I_{(\text{CH}_3/\text{H}_3\text{C})} \approx 10^4$ (this ratio becomes $\sim 10^3$ after correcting for small differences in the thicknesses of the organic films). We estimate that an interface having only van der Waals interactions is equivalent in its ability to pass current to a chain of approximately six transoid sigma bonds: that is $-\text{CH}_3/\text{H}_3\text{C}-$ is equivalent in its ability to pass current to a $-(\text{CH}_2)_6-$ unit. The smaller differences in the rates of electron transport across $-\text{CO}_2\text{H}\cdots\text{NH}_2-$ and $-\text{CO}_2\text{H}\cdots\text{HO}_2\text{C}-$ bridges that we observe are similar to those reported by Nocera et al.^[13] Beratan, Onuchic, and Betts^[17] developed theoretical models that fit experimentally determined rates of electron transfer in proteins to details of their structures, and inferred these orders of rates of tunneling: covalent > noncovalent bonds, and hydrogen bonds > van der Waals contacts. The agreement of our results with these limited experimental^[12–14] and theoretical data^[16, 17] suggests that the junction described here will be useful in quantifying these rates.

Theory: To fit the I – V curves, we have used two different theoretical models: the first assumes tunneling through a metal-insulator-metal junction; and the second assumes superexchange tunneling through a molecular bridge. The first approach is based on the Wentzel–Kramers–Brillouin (WKB) approximation for tunneling through an unstructured barrier, and gives a current density expressed by Equation (1), where ϕ_0 (in J) is the barrier height, V (in Volts) is the applied potential, m is the mass of an electron (in kg), \hbar is Planck's constant (in J s^{-1}) divided by 2π , e is the charge of an electron (in Coulombs) and d is the tunneling distance (in m).^[18]

$$I = \frac{e}{4\pi^2 \hbar d^2} \left\{ \left(e\phi_0 - \frac{eV}{2} \right) \exp \left[-\frac{2(2m)^{1/2}}{\hbar} \alpha \left(e\phi_0 - \frac{eV}{2} \right)^{1/2} d \right] - \left(e\phi_0 + \frac{eV}{2} \right) \exp \left[-\frac{2(2m)^{1/2}}{\hbar} \alpha \left(e\phi_0 + \frac{eV}{2} \right)^{1/2} d \right] \right\} \quad (1)$$

This model has been used successfully in the pioneering work of Mann and Kuhn.^[30] It is possible to extend the model for a rectangular potential barrier^[18] to barriers of parabolic shape^[19] by introducing an adjustable parameter, α , which is related to the shape of the barrier.^[19, 20] In this treatment, Equation (2) gives β . Fitting the I – V curves (Figure 2a) to Equation (1) for junctions in which SAM(1) consists of *n*-alkanethiolates gave an average value of $\alpha = 0.6$ and $\phi_0 = 2.5 \text{ eV}$. Introducing these values into Equation (2) gave a value of $\beta = 0.9 \text{ \AA}^{-1}$ at zero voltage, and a stronger voltage dependence than that observed experimentally over the range of 0.1 to 1 V.

$$\beta = -\frac{2(2m)^{1/2}}{\hbar} \alpha \left(e\phi_0 - \frac{eV}{2} \right)^{1/2} \quad (2)$$

The second theoretical model incorporates molecular structure into the tunneling barrier.^[21] This model considers

off-resonance tunneling of electrons across a single molecule in a metal-molecule-metal junction in response to the applied voltage. The model assumes a) that the molecules in the monolayer act independently, that is, the total current density is the product of the molecular current times the molecular density, and b) that the electrostatic potential profile is determined self-consistently through the combined solution of Poisson and Schrödinger equations.^[22] This model leads to an approximately constant electrostatic potential in the molecular bridge region, while the voltage drop occurs at the electrode–molecule interface. This approach gives Equation (3), where n is the number of molecules per unit area, N is the number of sites that compose a homogeneous molecular bridge, t is the transfer integral between sites, Δ_0 is the spectral density of either of the two electrodes at zero bias, and ϕ is the difference between the Fermi level of the electrode and the energy of each site. A “site” in this model is an atom or a group of atoms, whose orbital overlap provides the best superexchange pathway for electron transfer within a one-dimensional model.^[23] Equation (3) predicts 1) a power law dependence of the current on the applied potential; 2) an exponential dependence of the current on the length of the molecule L , where $I \propto e^{-\beta L}$ (β , derived from Equation (3), is given by Equation (4), for positive bias and $\phi < eV/2$); and 3) a much weaker dependence of β on V [Eq. (4)] compared to that from Equation (2).

$$I(V) = \frac{2e}{\pi\hbar} \frac{\Delta_0^2}{(1-2N)t} n \left\{ \left(\frac{e\phi + (eV/2)}{t} \right)^{1-2N} - \left(\frac{e\phi - (eV/2)}{t} \right)^{1-2N} \right\} \quad (3)$$

$$\beta = \frac{2}{a} \ln \left(\frac{e\phi - (eV/2)}{|t|} \right) \quad (4)$$

The fit of Equation (3) to the experimental I – V curve for $J_{\text{Ag-C}_{10}/\text{C}_{16}\text{-Hg}}$ ($d_{\text{Ag,Hg}} = 39 \text{ \AA}$), using ϕ , a , N , and t as adjustable parameters, gave physically reasonable values^[24, 25] for alkanes: $\phi = 4.8 \text{ V}$ and $t = -1.2 \text{ eV}$, for $N = 15$ and $a = 3 \text{ \AA}$. By using these values, Equation (4) gives a value of $\beta = 0.9 \text{ \AA}^{-1}$ that is approximately constant over the range 0–1 V. These characteristics of the calculated β value agree closely with our experimental observations. The value of a is larger than the average values of carbon–carbon distances in *trans*-extended alkyl chains, and the value of N is smaller than that expected if each site is defined as a carbon atom. One interpretation of these results is that each site corresponds to a methylene unit ($-\text{CH}_2-$) but that the dominant electron-transfer pathway is one that corresponds to “skipping” connecting CH_2 units.^[23] This interpretation amounts to mapping the zigzag geometry of a *trans*-extended alkyl chain onto a one-dimensional tight-binding (Hückel-type^[25] or ladder-type^[26]) chain. The calculated product of N and a is very close to the interelectrode separation.

As a whole, the experimental data fit Equation (3) quite well, particularly given the assumption that the total current is simply the product of the current/molecule by the number of molecules per cm^2 (5×10^{14}).^[27] The molecular structure of the tunneling barrier and the electrostatic potential enter naturally in this model, which does not require the parameter a invoked in the Simmons model.^[19] Furthermore, the barrier

value deduced from Equation (1) is too low compared with the experimental expectation.^[24]

Junctions $J_{\text{Ag-SAM}(1)/\text{SAM}(2)\text{-Hg}}$ have both advantages and disadvantages relative to other experimental systems as the basis for measurements of the influence of organic structure on rates of electron transport. Their advantages are that they: 1) are very easy to assemble and use; 2) are mechanically stable; 3) support a range of organic structures; 4) allow one electrode to be changed readily; 5) allow the direct correlation of electron transport and molecular structure. Their disadvantages are that they: 1) do not have the molecular-level resolution that makes measurements using scanning tunneling microscopy (STM)^[28] and break junctions^[29] so informative; 2) probably cannot be developed into practically useful microelectronic components; 3) are not compatible with measurements over a range of temperatures.

We believe that the combination of these junctions and the associated theory provide an experimentally straightforward and theoretically tractable system with which to explore the ability of thin films of organic molecules to support electron transport. This combination is a new tool for use in the development of organic microelectronics.

Experimental Section

Materials: Alkanethiols ($\text{HS}(\text{CH}_2)_{n-1}\text{CH}_3$ ($n = 8, 10, 12, 14, 16$)), thiophenol ($\text{HS}(\text{Ph})\text{H}$), and benzylthiol ($\text{HSCH}_2(\text{Ph})\text{H}$) were purchased from Aldrich or TCI and were used without further purification. Preparation of 4-biphenylthiol ($\text{HS}(\text{Ph})_2\text{H}$), 4-methylene-biphenylthiol ($\text{HSCH}_2(\text{Ph})_2\text{H}$), 4-triphenylthiol ($\text{HS}(\text{Ph})_3\text{H}$), and 4-methylene-triphenylthiol ($\text{HSCH}_2(\text{Ph})_3\text{H}$) was described previously.^[31–33] Hexadecane was purchased from Aldrich. Electronic grade mercury (99.9998%) was purchased from Alpha. **Caution:** Mercury is highly toxic.

SAMs on silver were prepared by immersing a freshly evaporated thin film of silver ($\text{Ag}(111)$; 2000 \AA) on a Si/SiO_2 wafer in a solution of the appropriate thiol (10 mm) in anhydrous ethanol (alkanethiols, thiophenol, and benzylthiol; the oligophenylene thiols) or THF (oligophenylene thiols) for 24 h. SAMs on mercury were formed by extruding a drop of liquid mercury from a capillary ($\sim 5 \mu\text{L}$) and exposing it to a solution of thiol (10 mm) in ethanol or hexadecane for ~ 10 min. The junctions were assembled as described previously.^[34] I – V curves were measured with the electrodes attached to an electrometer (Keithley 617 programmable electrometer) in two-electrode mode. During the measurement, the potential was increased in steps over the range of 0 to 1 V, or to the break-down voltage).

Received: March 9, 2001 [Z16738]

- [1] J. Jortner, M. A. Ratner, *Molecular Electronics* Blackwell, London, **1997**.
- [2] J. R. Winkler, H. B. Gray, *J. Biol. Inorg. Chem.* **1997**, *2*, 399–404.
- [3] C. C. Page, C. C. Moser, X. Chen, L. Dutton, *Nature* **1999**, *402*, 47–52.
- [4] M. A. Rampi, O. J. Shueller, G. M. Whitesides, *Appl. Phys. Lett.* **1998**, *72*, 1781–1783.
- [5] R. Haag, M. A. Rampi, R. E. Holmlin, G. M. Whitesides, *J. Am. Chem. Soc.* **1999**, *121*, 7895–7906.
- [6] J. W. Verhoeven, J. Kroon, M. N. Paddon-Row, A. M. Oliver in *Photoconversion Processes For Energy and Chemicals* (Eds.: D. O. Hall, G. Grassi), Elsevier, Amsterdam, **1989**.
- [7] A. Helms, D. Heiler, G. McLendon, *J. Am. Chem. Soc.* **1992**, *114*, 6227–6238.
- [8] J. F. Smalley, S. W. Feldberg, C. E. D. Chidsey, M. R. Linford, M. D. Newton, Y. Liu, *J. Phys. Chem.* **1995**, *99*, 13141–13149.

- [9] S. A. Domonte, M. Broge, *Chem. Phys. Lett.* **1998**, *290*, 136–142.
- [10] K. Slowiski, H. K. Y. Fong, M. Majda, *J. Am. Chem. Soc.* **1999**, *31*, 7257–7261.
- [11] J. L. Sessler, B. Wang, S. L. Springs, C. T. Brown in *Comprehensive Supramolecular Chemistry* (Ed.: M. Murakami), Oxford University Press, Oxford, **1996**, pp. 311–336.
- [12] K. Slowiski, R. V. Chamberlain, C. J. Miller, M. Majda, *J. Am. Chem. Soc.* **1997**, *119*, 11910–11919.
- [13] J. A. Roberts, J. P. Kirby, D. G. Nocera, *J. Am. Chem. Soc.* **1997**, *119*, 9230–9236.
- [14] P. J. F. DeRedge, S. A. Williams, M. J. Therien, *Science* **1995**, *269*, 1409–1413.
- [15] L. Yan, C. Marzolin, A. Terfort, G. M. Whitesides, *Langmuir* **1997**, *13*, 6704–6712.
- [16] A. Soudackov, S. Hammes-Schiffer, *J. Am. Chem. Soc.* **1999**, *121*, 10598–10607.
- [17] D. N. Beratan, J. N. Betts, J. N. Onuchic, *Science* **1991**, *252*, 1285–1288.
- [18] R. Wiesendanger, *Scanning Probe Microscopy and Spectroscopy*, Cambridge University Press, Cambridge, MA, USA, **1994**.
- [19] J. G. Simmons, *J. Appl. Phys.* **1963**, *34*, 1793–1832.
- [20] R. Holm, B. Kirchstein, *Z. Tech. Phys.* **1935**, *63*, 488–494.
- [21] V. Mujica, M. A. Ratner, *Chem. Phys.* in press.
- [22] V. Mujica, A. Roitberg, M. A. Ratner, *J. Chem. Phys.* **2000**, *112*, 6934–6839.
- [23] C. A. Naleway, L. A. Curtiss, J. R. Miller, *J. Chem. Phys.* **1991**, *95*, 8434.
- [24] M. Fujihira, H. Inokuchi, *Chem. Phys. Lett.* **1972**, *17*, 554–556.
- [25] L. Salem, *Molecular Orbital Theory of Conjugated Systems*, W. A. Benjamin, New York, **1966**.
- [26] R. Imhof, D. Antic, D. E. David, J. Michl, *J. Phys. Chem. A* **1997**, *101*, 4579–4586.
- [27] L. Yan, W. T. S. Huck, G. M. Whitesides in *Supramolecular Chemistry* (Ed.: A. Ciferri), Marcel Dekker, New York, **2000**, pp. 435–470.
- [28] W. Tian, S. Datta, S. Hong, R. Reifengerger, J. I. Henderson, C. P. Kubiak, *J. Chem. Phys.* **1998**, *109*, 2874–2882.
- [29] M. A. Reed, C. Zhou, C. J. Muller, T. P. Burgin, J. M. Tour, *Science* **1997**, *278*, 252–254.
- [30] B. Mann, H. Kuhn, *J. Appl. Phys.* **1971**, *42*, 4398–4405.
- [31] E. Sabatini, J. Cohen-Boulakia, M. Bruening, I. Rubinstein, *Langmuir* **1993**, *9*, 2974–2981.
- [32] Y.-T. Tao, C.-C. Wu, J.-Y. Eu, W.-L. Lin, *Langmuir* **1997**, *13*, 4018–4023.
- [33] H.-J. Himmel, A. Terfort, C. Wöll, *J. Am. Chem. Soc.* **1998**, *120*, 12069–12074.
- [34] R. Haag, M. A. Rampi, R. E. Holmlin, G. M. Whitesides, *J. Am. Chem. Soc.* **1999**, *121*, 7895–7906.

Quantitative Studies of Binding between Synthetic Galactosyl Ceramide Analogues and HIV-1 Gp120 at Planar Membrane Surfaces**

Yingmei Gu, Rachel LaBell, David F. O'Brien,* and S. Scott Saavedra*

The primary cellular receptor for the HIV-1 virus is CD4, a protein abundantly expressed on T cells. The HIV-1 viral envelope glycoproteins, gp120 (120 kD) and gp41 (41 kD) mediate the recognition and infection of CD4+ cells.^[1–3] However, in the early 1990s, it was discovered that HIV-1 can also infect CD4– cell lines, such as neural cells and epithelial cells.^[4,5] Galactosyl ceramide (GalCer), a glycosphingolipid (GSL) that is highly expressed in neural and intestinal tissues, is thought to be the alternate receptor to which gp120 binds to initiate the infection of CD4– cells.

Although the interaction between CD4 and gp120 has been extensively studied, relatively limited information has been obtained about the interaction between GSLs and gp120.^[6–14] In an effort to elucidate the relationship between gp120 binding activity and GSL structure, we previously investigated recombinant gp120 (rgp120) binding to several naturally occurring GSLs reconstituted into planar supported lipid bilayers by using total internal reflection fluorescence microscopy (TIRF).^[13] The presence of a carbohydrate on ceramide was shown to be required for rgp120 binding. Among the GSLs studied, galactosyl ceramide (GalCer) was the preferred receptor with respect to binding affinity, although rgp120 also recognized lactosyl ceramide (LacCer) and glucosyl ceramide (GlcCer). No attempt was made to investigate whether structural variations in the noncarbohydrate portion of the GSL (i.e. the ceramide) affected rgp120 binding.

Previous studies of protein binding to water-soluble receptors tethered to planar membranes have established that the structure of the nonreceptor portion of lipid is an important variable.^[15] For example, the efficiency of streptavidin binding to a biotin-conjugated lipid at a planar membrane surface is strongly influenced by the length of the spacer arm linking the biotin moiety to the lipid.^[16,17]

Herein we have assessed the influence of steric accessibility in rgp120–galactosyl recognition at a membrane surface. GalCer analogues with a water-soluble spacer arm of variable length between the galactosyl receptor and the lipophilic portion of the molecule were designed and synthesized. The analogues Gal-3, Gal-4, and Gal-5 were prepared by using tri(ethylene glycol), tetra(ethylene glycol), and penta(ethylene glycol) linkers, respectively. Each ethylene glycol unit adds approximately 3 Å to the length of the spacer arm. The lipophilic portion of each molecule is dioleoyl maleate. The

[*] Prof. Dr. D. F. O'Brien, Prof. Dr. S. S. Saavedra, Y. Gu, R. LaBell
Department of Chemistry, University of Arizona
Tucson, AZ, 85721-0041 (USA)
Fax: (+1) 520-621-8407
E-mail: dfobrien@u.arizona.edu, saavedra@u.arizona.edu

[**] This research was supported by the NIH (AI40359-02) and the NSF (CHE-9726132). Scientific discussions with Prof. Dr. J. C. Conboy (University of Utah) and Prof. Dr. J. Gervay-Hague (University of Arizona) are gratefully acknowledged.